

Review Article

Performance Analysis of Intra-Pulse Modulation Recognition of Radar Signals Via Hand-Crafted Feature Extraction and Classification

Narapusetti Adinarayana¹, CH Nagaraju²

^{1,2}Department of ECE, ANNAMACHARYA UNIVERSITY, New BoyanaPalli, Rajampet-516126, Annamayya District, Andhra Pradesh, India.

¹Corresponding Author : narapusetti.ece@gmail.com

Received: 15 November 2025

Revised: 04 February 2026

Accepted: 14 February 2026

Published: 29 April 2026

Abstract - Recognizing intrapulse-modulated signals is crucial for electronic warfare and reconnaissance systems since it involves identifying certain modulation patterns under weak and noisy signals. Recently, advances in feature extraction and signal processing have powered new techniques that greatly increase the identification speed and identification rate. Most approaches still only use crafted features and time-frequency representations for analyzing and classifying radar signals. In this article, we review the performance of such systems designed using handcrafted features and based on the recognition of different intra-pulse modulation. Most handcrafted systems still use the raw digital signal or the processed images of the time-frequency representation as feed for their algorithm. In this regard, we take the lead in the discussion by proposing a system for signal processing that transforms the raw signal into a time-frequency representation image to be processed. After the image is computed, it is passed on for a fixed feature set, followed by a set of standard classifiers for identification. In various test situations, our constructed pipeline showed consistent and significant improvement over established methods in terms of identification precision and overall accuracy.

Keywords - Intra-Pulse Modulation, Radar Signals, Feature extraction, Hand-crafted features, Classification.

1. Introduction

The Intra-Pulse Modulation (IPM) recognition serves as the foundation of modern radar processing, allowing analysts to identify different sources of radar while distinguishing the subtle differences in the pulse patterns of each emitter. Engineers decompose incoming waveforms into several components, looking for patterns of signatures marked within the pulse for automation in supporting electronic warfare, border patrol, and sea supervision as part of the automation engines. Because of the operation of embedded pulse IPM, reviewers have to rely on extensive scanning and variation modulation databases, which help to identify families of radar and their mission profiles [1]. When used with other classification methods, IPM profiling enhances discrimination, allowing operators to discern innocuous traffic from latent threats. These entire procedures show how meticulous, chronological, and routine analysis of radar returns provides considerable insights into the possible military and civilian purposes, along with the actionable strategies. Intra-Pulse Modulation (IPM) recognition serves as the foundation of modern radar processing, allowing analysts to identify different radar sources while distinguishing subtle differences in the pulse patterns of each emitter [2]. Radar

signal processing involves analyzing radar echoes and their features to extract useful information. The unobtrusive, yet vital, role of radar signal processing has been revolutionizing, and in a large number of cases, ensuring the safe and smooth execution, namely, guidance of military drones in hostile territories, air traffic control, and guidance of airplanes in and around heavily congested airports [3]. One of the most specialized functions in radar signal processing, radar emitter identification, attempts recognition of the novel signal by juxtaposing it against a catalogue of signal fingerprints - the inter-pulse modulation, or IPM pattern. Once an IPM pattern has been clearly established, reliable source identification and tagging can be made, which is so critically valuable for surveillance, and for defensive and offensive electronic warfare [4]. More general signal sorting, in terms of behaviour patterns, primitives, timing, jamming-resistant frequencies, and average power levels, needs to be done to allow systematic identification, like a librarian sorting signal reception into fiction, history, and reference. Once general sorting has been done, signal data is clean for systematic work to be done for IPM recognition, and intermediate coarse categorization translates into identification of probable emitters. Here, the technique of pulse compression, which is



radar signal compression, becomes an important tool, where it improves range resolution by enabling the shift of long signal compression to short and pulse compression to the echo, similar to a photographer focusing a lens to clear a background [5]. The rapidly evolving landscape of modern electronic warfare (EW) and cognitive radio has placed significant emphasis on the accurate identification of Radar Emission Signals (RES). A critical aspect of this identification is Intra-Pulse Modulation (IPM). Unlike simple pulse parameters such as duration or amplitude, intra-pulse modulation refers to deliberate changes in phase or frequency within a single pulse to improve range resolution and clutter rejection [6].

As radar systems become more sophisticated, employing techniques like Binary Phase Shift Keying (BPSK), Linear Frequency Modulation (LFM), and Polyphase codes (e.g., Frank, P1-P4), traditional time-domain analysis often falls short. In low Signal-to-Noise Ratio (SNR) environments, the temporal structure of these signals is easily obscured by noise, making direct classification nearly impossible [7].

By treating the radar pulse as an image, the problem shifts from signal processing to Computer Vision. This allows for the use of robust Feature Extraction algorithms that can identify unique geometric patterns—such as the diagonal line of an LFM signal or the "staircase" pattern of a Frequency Shift Keying (FSK) signal—within the TFI. In this manuscript, we experimentally investigate radar signals of intra-pulse modulation using both hand-crafted features and classical classifiers. Section 2 outlines the overall recognition methodology, and Section 3 presents the results of our recognition experiments on intra-pulse-modulated signals [8].

2. Literature Review

While deep learning has become a dominant force, hand-crafted feature extraction remains a vital approach for intra-pulse modulation (IPM) recognition. These methods are prized for their interpretability, lower computational requirements, and the fact that they do not require massive datasets to train. To conceal a modulation pattern within a compressed pulse, it is crucial to understand compression intimately, which is often the inverse Pulse Modulus (IPM). Analysts frequently utilize time-frequency representation, which is a powerful analytical technique, because it offers the ability to decompose a signal's energy into time and frequency components, thus allowing the analyst to detect certain subtle and fleeting elements that may otherwise go unnoticed. Radar operators, with the use of these integrated tools, are able to gather sufficient information to ascertain, identify, and, if required, engage airborne targets [9]. The versatility of time-frequency analysis enables it to serve as the foundation of many fields, such as communications, electronic warfare, and surveillance. Engineers working within tense scenarios understand that a single pulse is capable of curvature modulation on amplitude, frequency, and phase. To exploit such a pulse, teams often begin with hand-crafted feature sets,

which are simple and targeted fingerprints designed to capture each possible pulse swing. When these fingerprints are integrated with adaptive machine-learning models, the background noise level can be high, and the target signal can be weak, but the system will still be operational. The use of time-frequency representation drives the performance of modern radars, enabling them to detect and classify high drift waveforms in real time [10].

As previously stated, Wigner-Ville distribution and Fractional Fourier Transform techniques are applied to retrieve time-frequency representations of raw radar data to facilitate the detection of concealed patterns within the data [11, 12]. After capturing the radar data, they extract the parameters of how energy is distributed in time and frequency. This is important for cases where two or more modulations are close to overlapping [11, 12]. This involves the extraction of time and frequency parameters, energies, thereby making overlapping modulations easy to analyse. Central moments, energy-focusing efficiency, and similar statistics are then scanned to label the incoming signal. By providing a signal shape outline, they assist in data classification and shield the method from breakdown in situations of low Signal-to-Noise Ratio (SNR). This predominantly applies when many standard detectors fail, and the more novel geometry statistics are applicable [13].

In image recognition, hand-crafted features depend on deliberately defined algorithms that scan an image for hints, including edges, blobs, or color patches that assist subsequent steps that involve classifying, searching for, or naming images. Adjusting rules to focus on various image characteristics, such as texture, color, or shape, has contributed to many effective systems since the inception of computer vision. While the field is now dominated by deep-learning approaches, hand-crafted features continue to shine, especially when coupled with learned patterns, as their tailored expert knowledge tends to cover gaps and improve overall accuracy [14].

The following sections discuss, in recognition pipelines of the computational vision, how, where, and why. Among success stories illustrating this is in cloth-image-retrieval systems, where hand-crafted signatures consistently and accurately match textile samples from large collections. For one configuration dedicated to plaid fabrics, engineers combine local-binary-pattern cues with SIFT points and VLAD, providing a consistent description of a robust signature pattern. Evaluation of this signature demonstrates that the combination achieves such high precision and recall rates, especially in volume, that factory applications and production customers endorse the system, confirming that effective image features, crafted by hand and neural systems, still count and build on neural systems [15]. Tested and crafted features still matter in achieving accurate palmprint recognition. The Pixel Difference Vector technique focuses on

small clusters of adjacent pixels, evaluating the differences, and streamlining the whole image into a single histogram. PDV has surpassed many leading deep learning systems in lab testing as a testament to the benefits of having designs focused on specific problems [15].

The same spirit of resourcefulness appears in iris matching when edges blur or are unfocused. Filling in the missing pieces by targeting the entire periocular area—the skin surrounding the eye—improves accuracy. Hybrid systems that combine these rule-based features with outputs from a CNN are also beneficial for RGB-D object sorting. Incorporating explicit geometries with the learning of a deep net enables the model to handle problematic views and perform better on publicly available test datasets [16]. For face recognition, the integration of classical methods and deep learning approaches improves success rates, particularly in single-image galleries.

This technique captures fine texture impressions and shape indicators, which allows the system to endure rapid alterations in pose or illumination [17]. In light of this, several recent methods of feature mixing improve the performance of image classification by integrating handcrafted cues and CNN embeddings. Image recognition accuracy can be improved on some tasks by combining older techniques such as edge lines, texture maps, and contemporary deep learning CNNs [18]. Though interpretable, these cues will most likely not perform as well as deep networks on diverse, novel datasets because deep networks are far more adaptable to new patterns [12]. Feature design often requires considerable domain

knowledge, and the designed rules often fail when applied to situations far removed from their original context. Nevertheless, in some situations, such as millimetre-wave scans for person identification, torso-targeted descriptors are still more effective than fully learned end-to-end systems [19]. Hand-designed features, especially in recognition tasks, are not overshadowed by fully learned systems since, in most situations, they tend to refine the machine-generated tokens. From security to retail analytics, the sharpened classifiers broaden the range of application, and the classifiers improve, more applicable classifiers improve. Feature selection should be done to match the problem since the dataset and task goals will dictate the degree of improvement [20].

While hand-crafted features provide good results when identifying intra-pulse modulation, some disadvantages still exist. These features require expertise to develop, and often do not generalize well beyond the context for which they were constructed. Moreover, extracting and processing these features can be time and resource-intensive, which becomes a significant constraint for applications that require real-time computing. However, the use of hand-crafted features, combined with contemporary methods such as deep learning, greatly alleviates the trade-off between accuracy and speed of efficient computing [3]. In this manuscript, we experimentally investigate intra-pulse modulation in radar signals using both hand-crafted features and classical classifiers. Section 2 outlines the overall recognition methodology, and Section 3 presents the results of our recognition experiments on intra-pulse-modulated signals.

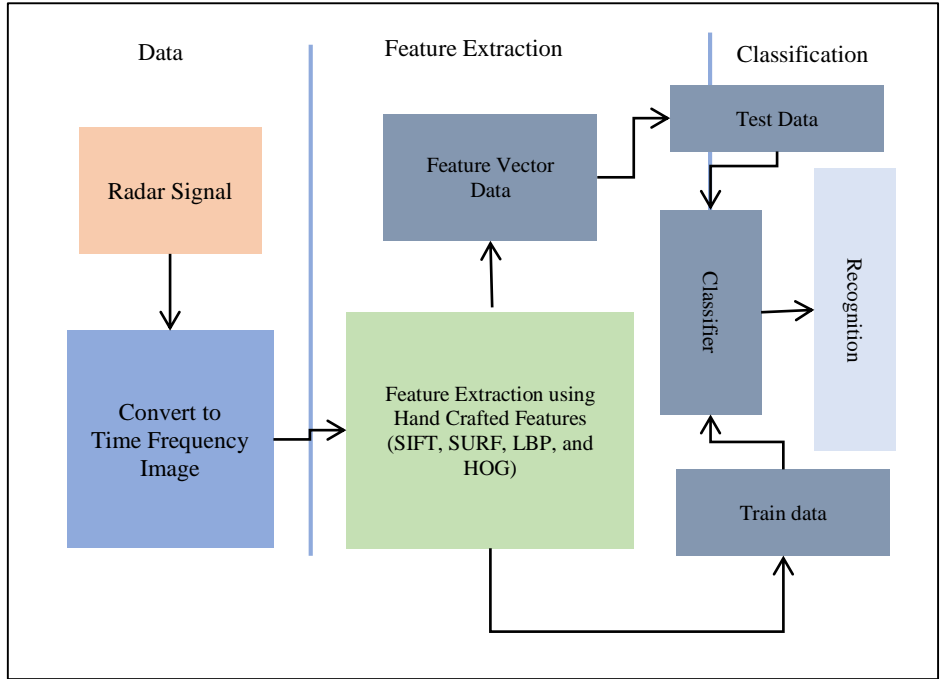


Fig. 1 Intra-pulse modulation recognition system using Hand-Crafted features

3. Methodology

This paper describes a system that recognizes intra-pulse

radar-modulation patterns by first extracting hand-crafted features and then passing those features to a range of classifiers, as shown in Figure 1. The main modes of intra-pulse radar modulation addressed here are phase modulation, frequency modulation, and combinations of the two. To test the system, a data set was built with the Low Probability of Intercept (LPI) Radar database 2025. The proposed system recognizes intra-pulse radar modulation patterns by converting radar signals into time–frequency images, extracting handcrafted features, and classifying the resulting feature vectors using multiple supervised classifiers. Figure 1 outlines the overall framework.

3.1. Time-Frequency Image Generation

Radar signals $x(t)$ are transformed into time–frequency representations $X(t,f)$ using the Short-Time Fourier Transform (STFT) defined as in Equation (1):

$$X(t, f) = \int_{-\infty}^{\infty} x(\tau)w(\tau - t)e^{-j2\pi f\tau} d\tau \quad (1)$$

where $X(t,f)$ is a window function centered at time t . The resulting spectrogram is obtained by computing the magnitude:

$$S(t, f) = |X(t, f)|^2 \quad (2)$$

This spectrogram $S(t,f)$ is used as a grayscale image representing the signal's energy distribution over time and frequency, serving as input to feature extraction algorithms [18].

3.2. Feature Extraction from Time–Frequency Images

3.2.1. Scale-Invariant Feature Transform (SIFT)

The Difference-of-Gaussian (DoG) pyramid in SIFT is used to detect keypoints by identifying extrema [21]. The DoG function $D(a, b, \sigma)$ is:

$$D(a, b, \sigma) = (G(a, b, k\sigma) - G(a, b, \sigma)) * I(a, b) \quad (3)$$

where $G(x, y, k\sigma)$ is a Gaussian blur with scale σ , and k is a constant multiplicative factor. Keypoints are refined by locating maxima/minima across scale-space and removing low-contrast points or edge responses. For each keypoint, a descriptor vector is computed by accumulating gradient magnitudes $m(a, b)$ and orientations $\theta(a, b)$ within localized neighborhoods:

$$m(a, b) = \sqrt{\frac{(I(a+1, b) - I(a-1, b))^2 + (I(a, b+1) - I(a, b-1))^2}{(I(a+1, b) - I(a-1, b))^2 + (I(a, b+1) - I(a, b-1))^2}} \quad (4)$$

$$\theta(a, b) = \tan^{-1} \left(\frac{I(a, b+1) - I(a, b-1)}{I(a+1, b) - I(a-1, b)} \right) \quad (5)$$

The descriptors are normalized to enhance robustness

against illumination changes.

3.2.2. Speeded-Up Robust Features (SURF)

SURF approximates DoG using box filters and integral images for fast computation [22]. The Hessian matrix $H(x, \sigma)$ determines interest points:

$$H(x, \sigma) = \begin{bmatrix} T_{xx}(x, \sigma) & T_{xy}(x, \sigma) \\ T_{xy}(x, \sigma) & T_{yy}(x, \sigma) \end{bmatrix} \quad (6)$$

where $\begin{bmatrix} T_{xx}(x, \sigma) & T_{xy}(x, \sigma) \\ T_{xy}(x, \sigma) & T_{yy}(x, \sigma) \end{bmatrix}$ are the convolution results of the image with second-order Gaussian derivatives. The determinant of the Hessian matrix approximates the blob response.

3.2.3. Local Binary Patterns (LBP)

LBP encodes texture by thresholding the neighbourhood of each pixel p_c with its center pixel intensity I_c :

$$LBP = \sum_{n=0}^{N-1} s(I_n - I_c)2^n, s(x) = \begin{cases} 1, & x \geq 0 \\ 0, & x < 0 \end{cases} \quad (7)$$

where I_n are the intensities of the N neighbouring pixels. The histogram of LBP codes over image patches forms a robust feature vector representing local texture [23].

3.2.4 Histogram of Oriented Gradients (HOG)

The image gradient at pixel (x,y) is computed as:

$$\begin{aligned} G_x &= I(x+1, y) - I(x-1, y), G_y \\ &= I(x, y+1) - I(x, y-1) \end{aligned} \quad (8)$$

Gradient magnitude and orientation are:

$$m(x, y) = \sqrt{G_x^2 + G_y^2}, \theta(x, y) = \tan^{-1} \left(\frac{G_y}{G_x} \right) \quad (9)$$

The image is divided into cells (e.g., 8×8 pixels), and a histogram of gradient orientations is calculated per cell, weighted by gradient magnitude. Normalization over spatial blocks enhances illumination invariance [24].

3.3. Classifier Design and Training

The extracted features are used to train and evaluate multiple classifiers for radar modulation identification.

3.3.1. Linear Regression (LR)

LR fits a linear model to map feature vectors \mathbf{x} to continuous outputs y :

$$y = \mathbf{w}^T \mathbf{x} + b \quad (10)$$

where w are weights and b is bias. Classification is achieved by thresholding or rounding outputs to discrete classes [25].

3.3.2. Logistic Regression (LOR)

LOR classifies feature vectors using a logistic sigmoid function:

$$P(y = 1|x) = \frac{1}{1+e^{-(w^T x+b)}} \quad (11)$$

Multiclass extension uses the softmax function for probability estimation across classes [26].

3.3.3. Decision Trees (DT)

DT recursively partitions feature space by selecting attribute thresholds that maximize information gain IG:

$$IG(D, a) = Entropy(D) - \sum_{v \in Values(a)} \frac{|D_v|}{|D|} Entropy(D_v) \quad (12)$$

Entropy is:

$$Entropy(D) = - \sum_{c=1}^C p_c \log_2 p_c \quad (13)$$

where p_c is the proportion of class c in dataset D .

3.3.4. Support Vector Machine (SVM)

SVM [27, 28] finds the optimal hyperplane $w^T \phi(x) + b = 0$ in a high-dimensional space defined by a kernel $\phi(x)$. The decision function is:

$$f(x) = \text{sign}(\sum_{i=1}^N \alpha_i y_i K(x_i, x) + b) \quad (14)$$

where α_i are Lagrange multipliers, y_i labels, and kernel K is often Radial Basis Function (RBF):

$$K(x_i, x_j) = \exp(-\gamma \|x_i - x_j\|^2) \quad (15)$$

3.3.5. Naïve Bayes (NB)

Given feature vector $x = (x_1, x_2, \dots, x_d)$, NB estimates posterior class probabilities assuming conditional independence:

$$P(C_k|x) \propto P(C_k) \prod_{j=1}^d P(x_j|C_k) \quad (16)$$

The class with the highest posterior is selected for classification [29].

3.3.6. k-Nearest Neighbors (KNN)

KNN predicts the class of x by majority voting among its k nearest neighbors in the training set using a distance metric $d(x, x_i)$, typically Euclidean:

$$d(x, x_i) = \sqrt{\sum_{j=1}^d (x_j - x_{ij})^2} \quad (17)$$

4. Results and Discussion

The Low Probability of Intercept (LPI) Radar database 2025 is a comprehensive dataset comprising 403,000 Time-Frequency Images (TFI) generated using multiple Time-Frequency Analysis (TFA) techniques such as the Smoothed Pseudo-Wigner-Ville Distribution (SPWVD), Choi-Williams Distribution (CWD), and Short-Time Fourier Transform (STFT). The images shown here are from MATLAB simulations, and they are being prepared for radar signal classification research. For this dataset, the same cross-validation methodology, bases of radar signal instances, and techniques of partitioning data were utilized as in previous studies for consistency and sound comparative analyses.

This database facilitates the creation and evaluation of classification techniques as it contains a significant assortment of synthetic LPI radar signals in the time-frequency domain. The focus is on research pertaining to the intercept radar systems with low probability, which evade detection from adversarial receivers through tactics like frequency agility, power control, and sophisticated signal processing. Researchers can leverage this dataset to improve signal recognition and detection accuracy and contribute to the enhancement of stealth radar technologies used in military and security applications.

The dataset illustrated in Figure 2 is divided into testing and training partitions (5675 TFI images) for classifier performance assessment. Metrics computed include precision, accuracy, recall, and F1-score. Classification results are compared against established radar signal recognition baselines to validate the efficacy of the handcrafted feature-classifier combination.

The experiments are performed using MATLAB 2024 with a system configured with an Intel Core Ultra 9 processor, NVIDIA GeForce RTX 5080 (16 GB), and 32 GB DDR5-5600 RAM. Quantitative evaluation is carried out using the confusion matrix. Quantitative evaluation results are tabulated in Tables 1, 2, and 3.

Quantitative evaluation results show that the histogram of gradient feature extraction techniques outperforms in intrapulse modulation recognition of radar signals using the mentioned classification techniques.

Both classifiers were tested on the same set of 2,665 images as in Table 1. In general, Linear Regression showed higher accuracy with LBP (86.3%) and HOG (87.0%), outperforming Logistic Regression in most cases except for HOG, where Logistic Regression achieved a comparable accuracy of 85.9%. Precision was highest for both classifiers using HOG features, with Logistic Regression reaching 90.0%, slightly ahead of Linear Regression's 89.1%.

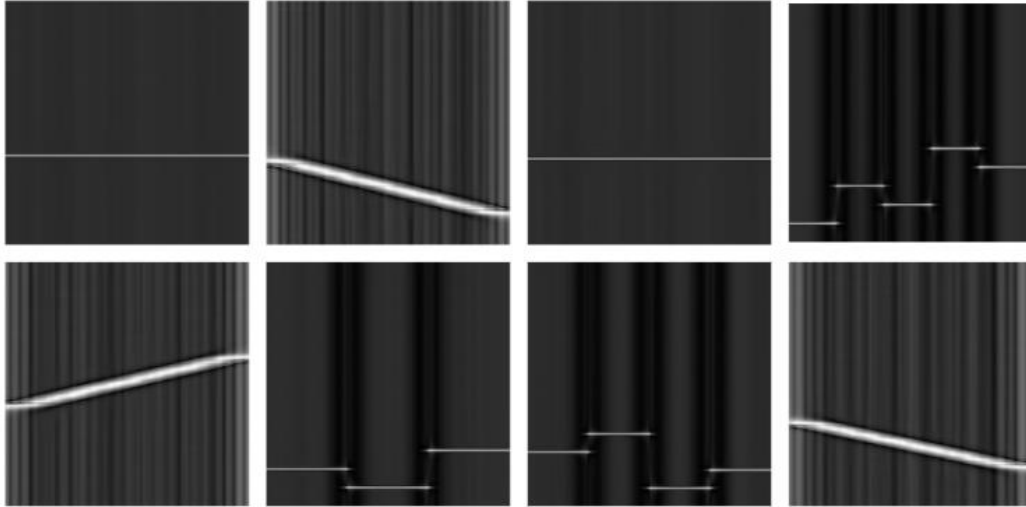


Fig. 2 The Low Probability of Intercept (LPI) Radar database 2025

Table 1. Performance evaluation of IPM Recognition of Radar Signals using Linear Regression and Logistic Regression classifiers

Measure	Classifier							
	Linear Regression (LR)				Logistic Regression (LOR)			
	SIFT	SURF	LBP	HOG	SIFT	SURF	LBP	HOG
Total Number of images tested	2665	2665	2665	2665	2665	2665	2665	2665
True Positive	1917	1767	1876	1886	1876	1898	1923	1954
True Negative	234	365	424	432	189	234	243	334
False Positive	391	421	228	231	321	336	312	218
False Negative	123	112	137	116	279	197	187	159
Accuracy	80.7	80.0	86.3	87.0	77.5	80.0	81.3	85.9
Precision	83.1	80.8	89.2	89.1	85.4	85.0	86.0	90.0

Table 2. Performance evaluation of IPM Recognition of Radar Signals using Naive Bayes and Support Vector Machine

Performance Measure	Classifier							
	Support Vector Machine (SVM)				Naive Bayes (NB)			
	SIFT	SURF	LBP	HOG	SIFT	SURF	LBP	HOG
Total Number of images tested	2665	2665	2665	2665	2665	2665	2665	2665
True Positive	1871	1862	1834	1896	1785	1774	1768	1734
True Negative	212	324	413	312	167	215	231	327
False Positive	373	415	234	216	213	321	324	206
False Negative	209	64	184	241	500	355	342	398
Accuracy	78.2	82.0	84.3	82.9	73.2	74.6	75.0	77.3
Precision	83.4	81.8	88.7	89.8	89.3	84.7	84.5	89.4

Table 3. Performance evaluation of IPM Recognition of Radar Signals using K-Nearest Neighbors and Decision Tree

Performance Measure	Classifier							
	Decision Tree (DT)				K-Nearest Neighbors (KNN)			
	SIFT	SURF	LBP	HOG	SIFT	SURF	LBP	HOG
Total Number of images tested	2665	2665	2665	2665	2665	2665	2665	2665
True Positive	1867	1893	1847	1863	1645	1864	1754	1843
True Negative	224	243	268	301	213	227	245	312
False Positive	324	297	268	144	313	267	247	134
False Negative	250	232	282	357	494	307	419	376
Accuracy	78.5	80.2	79.4	81.2	69.7	78.5	75.0	80.9
Precision	85.2	86.4	87.3	92.8	84.0	87.5	87.7	93.2

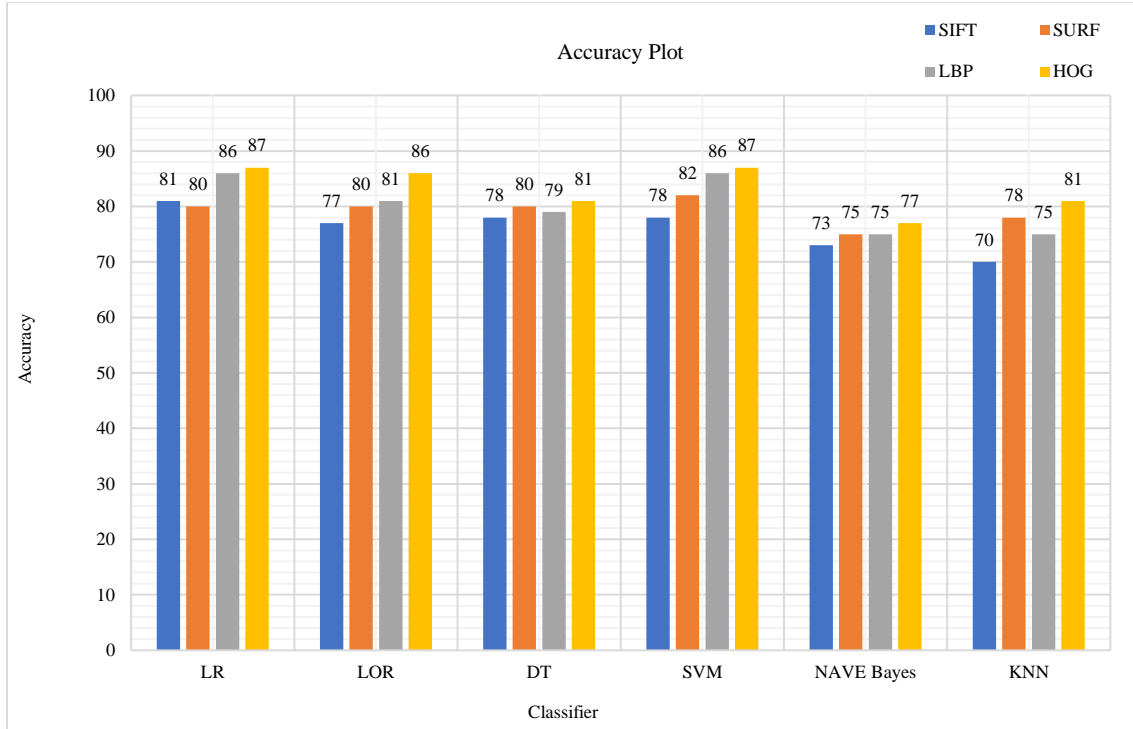


Fig. 3 Performance evaluation accuracy plot of IPM Recognition of Radar Signals using handcrafted features and classifiers

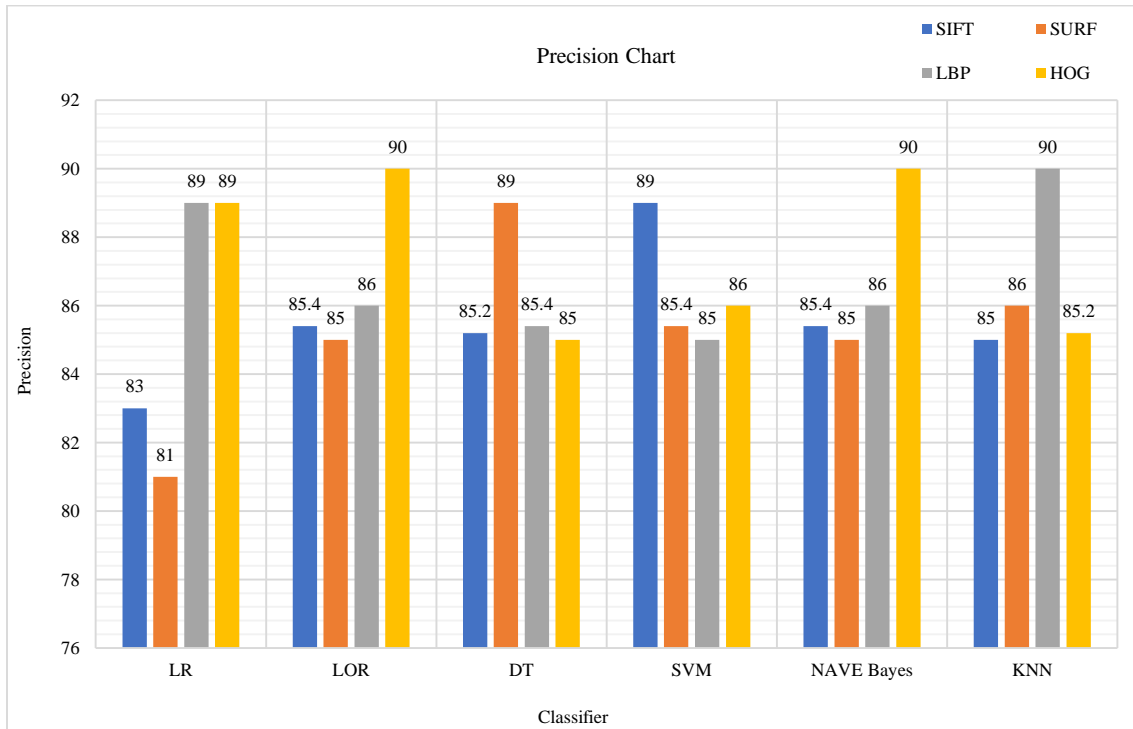


Fig. 4 Performance evaluation precision plot of IPM Recognition of Radar Signals using handcrafted features and classifiers

True positives were generally higher with Linear Regression in SIFT and SURF, while Logistic Regression had an edge in HOG. Linear Regression demonstrated superior performance among all features with respect to True

Negatives, indicative of an improved detection rate with no unnecessary alarms being signalled. Moreover, Linear Regression evidenced fewer false positives and false negatives. This indicates that it was better balanced and more

adept at discerning the different classes as compared to other classifiers. Overall, and with the features derived from both LBP and HOG, Linear Regression was noted to maintain an improved degree of accuracy and an overall balanced performance. This was contrasted with the more competitive performance expressed by Logistic Regression on the HOG features. This was most clearly refined in its precision. As presented in Table 2, SVM obtained the greatest accuracy of all classifiers, including Naive Bayes, and this was achieved on the LBP features with an accuracy of 84.3%, as well as having commendable results with SURF and HOG. Although Naive Bayes evidenced lower accuracy overall, in some situations, especially with SIFT and HOG, it evidenced noteworthy precision along with accuracy, which resulted in an 89% true precision and above toward the most positive class. SVM accounted for all the true positives, and Naive Bayes accounted for the most false negatives; thus, SVM was the most adept in obtaining all of the positive cases. True negatives were also better for SVM, indicating fewer false alarms overall. Naive Bayes was presented with a precision defect for the overall accuracy.

Thus, SVM was the most accurate and balanced classifier, while Naive Bayes was precise, yet suffered from a lack of consistency in classification. Table 3 indicates that the Decision Tree achieved consistently solid accuracy with all features, reaching an 81.2% peak with HOG. It continued to boast high accuracy, especially with HOG (92.8%). Unlike KNN, which recorded a narrower accuracy range that began with SIFT at a lower 69.7% and improved to 80.9% with HOG, KNN also achieved strong precision, 93.2% with HOG. DT had fewer false negatives overall, implying that they were better at detecting true positives, whereas KNN had a greater struggle with false negatives, especially on SIFT. Although both performed HOG features the best, DT's accuracy was more consistent compared to KNN across the other feature sets.

As illustrated in Figure 3, HOG and LBP features typically resulted in the highest accuracy for the majority of the classifiers. HOG and LBP enabled LR, SVM, and LOR to achieve the best results with accuracy in the mid to high 80s. DT and KNN showed consistent and lower overall accuracy, with HOG being the highest. Naive Bayes consistently dropped in accuracy across all features, especially with SIFT. In summary, HOG features emerged as the top option for increasing classifier accuracy on all counts. Most classifiers and features have high precision scores, primarily within the

80-90% range. Analysis of Figure 4 indicates that HOG and LBP features are the most influential in increasing precision, with LR and Naive Bayes reaching approximately 90% precision on HOG. KNN achieves its highest precision with LBP (90%). SVM and LR also perform admirably on HOG and LBP. DT consistently holds precision in the mid-80s for all features. Altogether, precision does not vary greatly with the choice of features, although HOG and LBP are the more influential parameters in the set of hand-crafted features.

5. Conclusion

In this work, Intra-pulse modulation recognition of radar signals is experimentally analyzed using various handcrafted features and classifiers. Handcrafted features such as SIFT, SURF, LBP, and HOG are used for feature extraction and dataset generation. LR, LOR, DT, SVM, Naive Bayes, and KNN classifiers are tested with hand-crafted feature datasets. The examination of precision across the classifiers shows that all methods achieve high levels, clustering mostly between 80 percent and 90 percent, which points to their strong ability to label positive cases correctly. Logistic Regression and Naive Bayes achieved their maximum precision (90%) with HOG features. This indicates that HOG features increase these models' reliability. K-Nearest Neighbors obtained a 90 percent precision with LBP features, and the highest precision for the Support Vector Machine was achieved with SIFT descriptors. The Decision Tree, however, remained constant in the mid-80s range, showing minimal change irrespective of the features used.

Overall, the classifiers demonstrate competent performance. However, model and descriptor combinations that contain HOG or LBP increase precision meaningfully. The accuracy of the classifiers supports this conclusion, showing a strong relationship between feature extraction and classifier performance. HOG and LBP provide the highest accuracy in most algorithms. The Support Vector Machine and Linear Regression obtain their peak accuracy of 87.0 percent with HOG, and Logistic Regression also exceeds 80 percent with HOG or LBP. The Decision Tree and K-Nearest Neighbours, like the Decision Tree, also improve with HOG. Although Naive Bayes continues to provide the lowest accuracy, this gap steadily declines as more advanced, especially HOG, features are used. When considering all the evidence, the Histogram of Oriented Gradients method has unambiguously proven to be the most effective feature-extraction method for improving classification accuracy, regardless of the algorithms used.

References

- [1] Wu Shunjun, Liao Guisheng, and Bao Zheng, "Advanced Technology on Radar Signal Processing," *2001 CIE International Conference on Radar Proceedings (Cat No.01TH8559)*, Beijing, China, pp. 16-19, 2001. [[CrossRef](#)] [[Google Scholar](#)] [[Publisher Link](#)]
- [2] Bachir Jdid et al., "Robust Automatic Modulation Recognition through Joint Contribution of Hand-Crafted and Contextual Features," *IEEE Access*, vol. 9, pp. 104530-104546, 2021. [[CrossRef](#)] [[Google Scholar](#)] [[Publisher Link](#)]

- [3] Byungkoo Park, and Jae Min Ahn, "Intra-Pulse Modulation Recognition using Pulse Description Words and Complex Waveforms," *2017 International Conference on Information and Communication Technology Convergence (ICTC)*, Jeju, Korea (South), pp. 555-560, 2017. [[CrossRef](#)] [[Google Scholar](#)] [[Publisher Link](#)]
- [4] Yue Qi et al., "Handcrafted and Neural Network-based Features for Outlier Modulation Detection," *2022 56th Asilomar Conference on Signals, Systems, and Computers*, Pacific Grove, CA, USA, pp. 698-702, 2022. [[CrossRef](#)] [[Google Scholar](#)] [[Publisher Link](#)]
- [5] Hui Ning, and Chao Chen, "Recognition of Intra-Pulse Signals Modulation based on Fractional Fourier Transform," *Dianxun Jishu/ Telecommunications Engineering*, vol. 51, no. 12, pp. 42-47, 2011. [[Google Scholar](#)]
- [6] Mark A. Richards, *Fundamentals of Radar Signal Processing*, New York: McGraw-Hill, vol. 1, 2005. [[Google Scholar](#)]
- [7] Mourad Barkat, *Signal Detection and Estimation*, 2nd ed., Artech, 2005. [[Google Scholar](#)] [[Publisher Link](#)]
- [8] Boualem Boashash, *Time-Frequency Signal Analysis and Processing: A Comprehensive Reference*, 2nd ed., Academic Press, 2016. [[Google Scholar](#)] [[Publisher Link](#)]
- [9] Guo-bing HU et al., "Intrapulse Modulation Recognition of Signals based on Statistical Test of Energy Focusing Efficiency," *Editorial Department of Journal on Communications*, vol. 34, no. 6, pp. 136-145, 2013. [[Google Scholar](#)] [[Publisher Link](#)]
- [10] Tao Chen et al., "Radar Signal Intra-Pulse Modulation Recognition based on Point Cloud Network," *IEEE Signal Processing Letters*, vol. 32, pp. 596-600, 2025. [[CrossRef](#)] [[Google Scholar](#)] [[Publisher Link](#)]
- [11] Zhiyu Qu et al., "Radar Signal Intra-Pulse Modulation Recognition based on Convolutional Neural Network and Deep Q-Learning Network," *IEEE Access*, vol. 8, pp. 49125-49136, 2020. [[CrossRef](#)] [[Google Scholar](#)] [[Publisher Link](#)]
- [12] Ning Dong et al., "Intrapulse Modulation Radar Signal Recognition using CNN with Second-Order STFT-based Synchrosqueezing Transform," *Remote Sensing*, vol. 16, no. 14, pp. 1-13, 2024. [[CrossRef](#)] [[Google Scholar](#)] [[Publisher Link](#)]
- [13] Zhiyu Qu et al., "Radar Signal Intra-Pulse Modulation Recognition based on Convolutional Denoising Autoencoder and Deep Convolutional Neural Network," *IEEE Access*, vol. 7, pp. 112339-112347, 2019. [[CrossRef](#)] [[Google Scholar](#)] [[Publisher Link](#)]
- [14] Xinjie Ju et al., "Radar Signal Recognition based on Time-Frequency Feature Extraction and Convolutional Neural Network," *Second International Conference on Digital Society and Intelligent Systems (DSInS 2022)*, vol. 12599, pp. 557-563, 2023. [[CrossRef](#)] [[Google Scholar](#)] [[Publisher Link](#)]
- [15] Kuiyu Chen et al., "Modulation Recognition of Radar Signals based on Adaptive Singular Value Reconstruction and Deep Residual Learning," *Sensors*, vol. 21, no. 2, pp. 1-17, 2021. [[CrossRef](#)] [[Google Scholar](#)] [[Publisher Link](#)]
- [16] Chenkai Wang, and Lei Kuang, "Recognition of Radar In-Pulse Modulation based on Radar De-Noiseing Linknet," *2022 2nd International Conference on Computer Science, Electronic Information Engineering and Intelligent Control Technology (CEI)*, Nanjing, China, pp. 233-236, 2022. [[CrossRef](#)] [[Google Scholar](#)] [[Publisher Link](#)]
- [17] Fatih Çağatay Akyön et al., "Deep Learning in Electronic Warfare Systems: Automatic Intra-Pulse Modulation Recognition," *2018 26th Signal Processing and Communications Applications Conference (SIU)*, Izmir, Turkey, pp. 1-4, 2018. [[CrossRef](#)] [[Google Scholar](#)] [[Publisher Link](#)]
- [18] Wang Yuzhang, "Method for Recognizing Intrapulse Modulation Types of Radar Signals," *2024 IEEE 2nd International Conference on Control, Electronics and Computer Technology (ICCECT)*, Jilin, China, pp. 159-163, 2024. [[CrossRef](#)] [[Google Scholar](#)] [[Publisher Link](#)]
- [19] Yanping Liao, and Nongkai Tian, "Radar Intra-Pulse Modulation Signal Recognition using Multi-Branch Denoising Convolutional Neural Network and Inception-ResN et-v2," *2024 9th International Conference on Electronic Technology and Information Science (ICETIS)*, Hangzhou, China, pp. 396-402, 2024. [[CrossRef](#)] [[Google Scholar](#)] [[Publisher Link](#)]
- [20] Jingyue Liang, Zhongtao Luo, and Renlong Liao, "Intra-Pulse Modulation Recognition of Radar Signals based on Efficient Cross-Scale Aware Network," *Sensors*, vol. 24, no. 16, pp. 1-17, 2024. [[CrossRef](#)] [[Google Scholar](#)] [[Publisher Link](#)]
- [21] David G. Lowe, "Distinctive Image Features from Scale-Invariant Keypoints," *International Journal of Computer Vision*, vol. 60, no. 2, pp. 91-110, 2004. [[CrossRef](#)] [[Google Scholar](#)] [[Publisher Link](#)]
- [22] Herbert Bay, Tinne Tuytelaars, and Luc Van Gool, "Surf: Speeded Up Robust Features," *Computer Vision -- ECCV 2006: 9th European Conference on Computer Vision*, Graz, Austria, vol. 3951, pp. 404-417, 2006. [[CrossRef](#)] [[Google Scholar](#)] [[Publisher Link](#)]
- [23] Timo Ojala, Matti Pietikäinen, and David Harwood, "A Comparative Study of Texture Measures with Classification based on Featured Distributions," *Pattern Recognition*, vol. 29, no. 1, pp. 51-59, 1996. [[CrossRef](#)] [[Google Scholar](#)] [[Publisher Link](#)]
- [24] N. Dalal, and Bill Triggs, "Histograms of Oriented Gradients for Human Detection," *2005 IEEE Computer Society Conference on Computer Vision and Pattern Recognition (CVPR'05)*, San Diego, CA, USA, vol. 1, pp. 886-893, 2005. [[CrossRef](#)] [[Google Scholar](#)] [[Publisher Link](#)]
- [25] Andrew Gelman, and Jennifer Hill, *Data Analysis using Regression and Multilevel/Hierarchical Models*, Cambridge University Press, New York, 2006. [[Google Scholar](#)] [[Publisher Link](#)]
- [26] David W. Hosmer Jr, Stanley Lemeshow, and Rodney X. Sturdivant, *Applied Logistic Regression*, John Wiley and Sons, 2013. [[CrossRef](#)] [[Google Scholar](#)] [[Publisher Link](#)]
- [27] Leo Breiman et al., *Classification and Regression Trees*, 1st ed., Chapman and Hall/CRC, New York, 1984. [[CrossRef](#)] [[Google Scholar](#)] [[Publisher Link](#)]

- [28] Corinna Cortes, and Vladimir Vapnik, "Support-Vector Networks," *Machine Learning*, vol. 20, no. 3, pp. 273-297, 1995. [[CrossRef](#)] [[Google Scholar](#)] [[Publisher Link](#)]
- [29] Harry Zhang, "The Optimality of Naive Bayes," *Proceedings of the Seventeenth International Florida Artificial Intelligence Research Society Conference*, The AAAI Press, Menlo Park, California, pp. 1-6, 2004. [[Google Scholar](#)] [[Publisher Link](#)]